Inorg. Chem. **2005**, *44*, 2570–2572

Spin Density Distribution in Five- and Six-Coordinate Iron(II)–Porphyrin NO Complexes Evidenced by Magnetic Circular Dichroism Spectroscopy

V. K. K. Praneeth,[†] Frank Neese,[‡] and Nicolai Lehnert*,[†]

Institut für Anorganische Chemie, Christian-Albrechts-Universität Kiel, Olshausenstrasse 40, 24098 Kiel, Germany, and Max-Planck Institut für Bioanorganische Chemie, Stiftstrasse, 34-36, 45470 Mülheim an der Ruhr, Germany

Received January 28, 2005

Using magnetic circular dichroism (MCD) spectroscopy together with DFT calculations, the spin density distributions in five-coordinate [Fe(TPP)(NO)] (**I**) and six-coordinate [Fe(TPP)(MI)(NO)] (**II**, MI = 1-methylimidazole) are defined. In the five-coordinate complex, a strong Fe–NO σ bond between π^*_h and d_{z^2} is present that leads to a large transfer of spin density from the NO ligand to Fe(II) corresponding to an electronic structure with noticeable Fe(I)–NO^+ character. Consequently, the MCD spectrum is dominated by paramagnetic **C**-term contributions. On coordination of the sixth ligand, the spin density is pushed back from the iron toward the NO ligand, resulting in an Fe(II)–NO(radical) type of electronic structure. This is reflected by the fact that the MCD spectrum is dominated by diamagnetic contributions.

Iron−porphyrin NO complexes play a key role in the mechanisms of many metalloproteins.[1,2] Hence, synthetic model systems for these species have been investigated in great detail.[3] Corresponding iron(II)−NO complexes are still the focus of many ongoing studies because of their interesting spectroscopic and photochemical properties[4] and their mechanistic significance.[3] In this communication, the low-temperature magnetic circular dichroism (MCD) spectra of five-coordinate [Fe^{II}(TPP)(NO)] (**I**, TPP = tetraphenylporphyrin) and six-coordinate [Fe^{II}(TPP)(MI)(NO)] (**II**, MI = 1-methylimidazole) are reported for the first time and analyzed with the help of density functional (DFT) calculations. Both complexes **I** and **II** have $S = {}^1/_2$ ground states.[5] From their different EPR spectra, Wyllie et al. speculated that these systems have different electronic ground states,[6] but no further evidence for this conjecture is provided. Judging from the MCD spectra and DFT calculations presented here, this difference in electronic structure of **I** and **II** is elucidated.

MCD intensity is generally considered to arise from three different mechanisms.[7] The **C** term is temperature-dependent and originates from spin−orbit coupling of the ground and target excited states with other intermediate excited states. On the other hand, the **A** and **B** terms are temperature-independent and are also present in diamagnetic materials. Thus, the paramagnetic (**C**-term) contribution to the total spectrum can be extracted by subtracting MCD data taken at variable temperatures. Figure 1 shows the MCD spectra of five-coordinate (5C) [Fe^{II}(TPP)(NO)] (top) and six-coordinate (6C) [Fe^{II}(TPP)(MI)(NO)] (bottom) in comparison. As one can see, these data are very different. In the case of **I**, the **C**-term spectrum obtained from temperature-dependent data is identical in appearance to the total spectrum. Consequently, the MCD response is dominated by the paramagnetic **C**-term contribution. Because spin−orbit coupling is weak for light elements such as carbon, nitrogen, and oxygen, the **C**-term nature of the spectrum indicates that a significant amount of spin density of the unpaired electron in **I** must be located on the formally iron(II) center. This is dramatically different for the 6C complex **II**. From Figure 1, bottom, one can see that the deconvoluted MCD **C**-term spectrum is different from the total spectrum, which is, in fact, dominated by temperature-independent diamagnetic contributions (**A** and **B** terms). These are generally observed for diamagnetic metal porphyrin complexes because of the occurrence of (practically) degenerate excited states in the porphyrin dianion with approximate D_{4h}

* To whom correspondence should be addressed. E-mail: nlehnert@ac.uni-kiel.de.
[†] Christian-Albrechts-Universität Kiel.
[‡] Max-Planck Institut für Bioanorganische Chemie.

(1) McCleverty, J. A. *Chem. Rev.* **2004**, *104*, 403.
(2) (a) Richardson, D. J.; Watmough, N. J. *Curr. Opin. Chem. Biol.* **1999**, *3*, 207. (b) Ding, X. D.; Weichsel, A.; Andersen, J. F.; Shokhireva, T. K.; Balfour, C.; Pierik, A. J.; Averill, B. A.; Montfort, W. R.; Walker, F. A. *J. Am. Chem. Soc.* **1999**, *121*, 128. (c) Poulos, T. L.; Li, H.; Raman, C. S. *Curr. Opin. Chem. Biol.* **1999**, *3*, 131.
(3) (a) Ford, P. C.; Lorkovic, I. M. *Chem. Rev.* **2002**, *102*, 993. (b) Wyllie, G. R. A.; Scheidt, R. *Chem. Rev.* **2002**, *102*, 1067.
(4) Cheng, L.; Novozhilova, I.; Kim, C.; Kovalevsky, A.; Bagley, K. A.; Coppens, P.; Richter-Addo, G. B. *J. Am. Chem. Soc.* **2000**, *122*, 7142.
(5) Westcott, B. L.; Enemark, J. H. *Transition Metal Nitrosyls*; Solomon, E. I., Lever, A. B. P., Eds.; Wiley: New York, 1999; Vol. 2, pp 403−450.
(6) Wyllie, G. R. A.; Schulz, C. E.; Scheidt, W. R. *Inorg. Chem.* **2003**, *42*, 5722.
(7) (a) Cheesman, M. R.; Greenwood, C.; Thomson, A. J. *Adv. Inorg. Chem.* **1991**, *36*, 201. (b) Neese, F.; Solomon, E. I. *Inorg. Chem.* **1999**, *38*, 1847. (c) Oganesyan, V. S.; George, S. J.; Cheesman, M. R.; Thomson, A. J. *J. Chem. Phys.* **1999**, *110*, 762.

10.1021/ic050144k CCC: $30.25
Published on Web 03/12/2005

Table 1. Comparison between Experimental and Calculated Properties of Fe(II)−Porphyrin NO Adducts (All $S = {}^1/_2$) [a]

molecule	geometric parameters (Å or deg) Fe−N	N−O	Fe−N−O	Fe−X	ν(N−O) (cm^{-1})	spin density[b] Fe	NO	Mössbauer parameters (mm/s) δ	ΔE_q	EPR parameters g_{max}	g_{mid}	g_{min}	orientation	ref
Fe(TPP)(NO) (**I**)[c]	1.72	1.12	149	−	1697			0.33[a]	1.25[a]	2.102	2.064	2.010	−	11a
Fe(OEP)(NO)[c]	1.73	1.17	143	−	1673[a]			0.35[a]	1.26[a]	2.106	2.057	2.015	g_{min}/Fe−N = 8°	11b
Fe(P)(NO) (**Ia**) BP86/TZVP	1.70	1.18	146	−	1703	+0.47	+0.53			2.043	2.007	1.997	g_{min}/Fe−N = 24°	
Fe(P)(NO)[d]								0.36	0.73	2.049	2.025	2.004	g_{min}/Fe−N = 20°	
Fe(TPP)(MI)(NO) (**II**)[c]	1.75	1.18	138	2.17	1630			0.34[a]	0.73[a]	2.079	2.004	1.972	−	11d
Fe(P)(MI)(NO) (**IIa**) BP86/TZVP	1.73	1.19	140	2.18	1662	+0.21	+0.78			2.031	1.998	1.972	g_{mid}/Fe−N = 41° g_{min}/Fe−N = 49°	
Fe(P)(MI)(NO)[d]								0.38	|0.57|	2.024	1.991	1.955	g_{mid}/Fe−N = 29°	

[a] For abbreviations, see text. Fe−X is the Fe−N(imidazole) distance. Because there is an ambiguity about the N−O stretch in five-coordinate [Fe(TPP)(NO)] (values of 1700[11a] and 1670[3b] cm^{-1} have been reported), we have reinvestigated the IR spectra of **I** and **II** as shown in Figure S3. For [Fe(OEP)(NO)], ν(N−O) is taken from ref 6. Experimental Mössbauer parameters are taken from ref 6. [b] Spin densities are calculated at the B3LYP/LanL2DZ* level (cf. Experimental Details in the Supporting Information). [c] Structural data: [Fe(TPP)(NO)] and [Fe(OEP)(NO)], ref 3b; [Fe(TPP)(MI)(NO)], ref 6. [d] Calculated with B3LYP and the following basis sets: Fe, CP(PPP); N, EPR−II; C and O, TZVP; H, TZV (see Supporting Information).

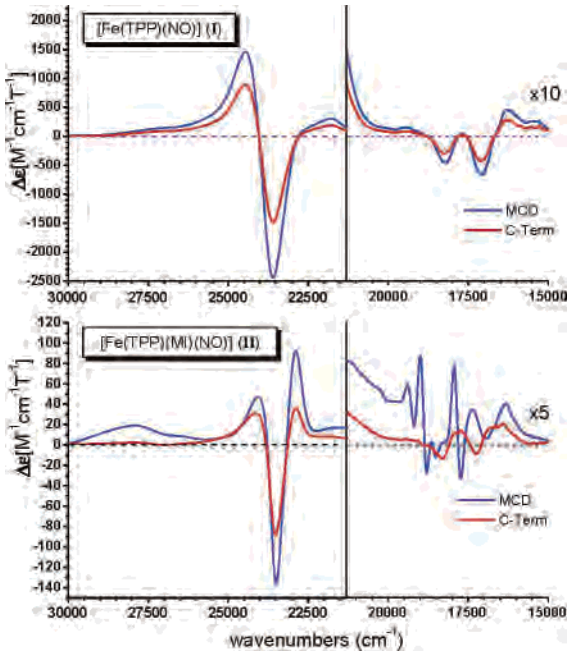

Figure 1. MCD spectra of [Fe^{II}(TPP)(NO)] (top) and [Fe^{II}(TPP)(MI)(NO)] (bottom) measured in a butyronitrile/propionitrile glass.

symmetry.[8] This indicates that the unpaired spin density is mostly located on the NO unit in the 6C case, which leads to the temperature-independent MCD spectrum of diamagnetic low-spin Fe(II)−porphyrins. Detailed assignments of the observed electronic transitions are complicated and will therefore be presented in a forthcoming full paper.

The fact that the paramagnetic complex **II** exhibits such low **C**-term intensity is surprising and indicates a different ground state for **II** compared to **I**. To elucidate the electronic structural origin of this difference, DFT calculations at the BP86/TZVP level have been applied using the model systems [Fe^{II}(P)(NO)] (**Ia**) and [Fe^{II}(P)(NO)(MI)] (**IIa**, P = porphine; cf. Figure S4, Supporting Information).[9] As shown in Table 1, the obtained agreement between the calculated and experimental structures is excellent. In complex **II**, the Fe−NO bond is dominated by two interactions. First, a pseudo-σ donation from the singly occupied π^*_h orbital of NO (h = horizontal, the π^* orbital in the Fe−N−O plane) into the unoccupied d_{z^2} orbital of iron(II) is present.[9] The corresponding bonding combination, $\alpha\langle 123\rangle$, has an additional admixture of d_{xz} and is therefore labeled $\pi^*_h\_d_{z^2}/d_{xz}$. It is the HOMO of **II** (cf. Figure 2, left). Because d_{z^2} also interacts with the σ donor orbital of the bound 1-methylimidazole, this competition for d_{z^2} explains the strong trans effect of NO on σ-donor ligands. This can also

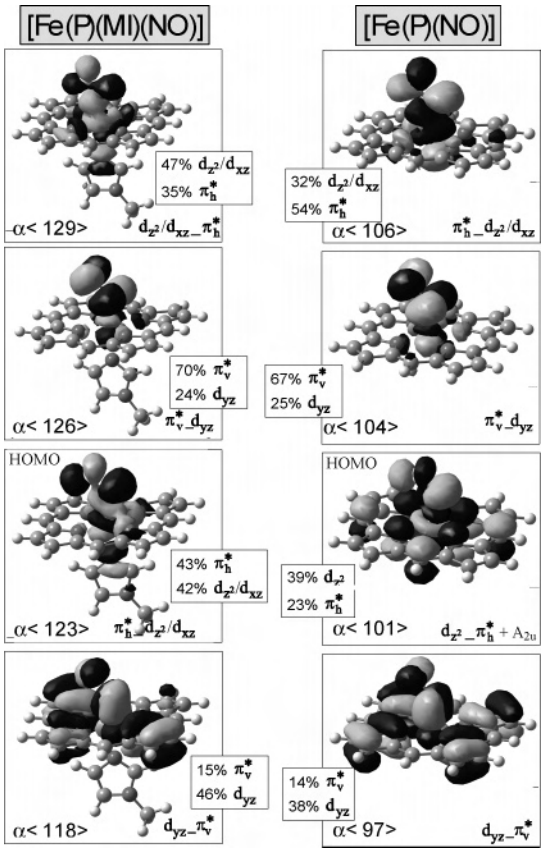

Figure 2. Contour plots of important α-MOs of [Fe^{II}(P)(MI)(NO)] (left) and [Fe^{II}(P)(NO)] (right) calculated with BP86/TZVP.

(8) Gouterman, M. Optical Spectra and Electronic Structure of Porphyrins and Related Rings. In *The Porphyrins*; Dolphin, D., Ed.; Academic Press: New York, 1978; Vol. III.

(9) The model systems and the applied coordinate system are shown in Figure S4. The complete MO diagram and contour plots of **II** are shown in Figures S6 and S7.

be seen from the corresponding antibonding orbital, $d_{z^2}/d_{xz}\_\pi^*_h$ ($\alpha\langle 129\rangle$). The second interaction is a medium-strength π back-bond between the π^*_v orbital of NO (v = vertical, the π^* orbital perpendicular to the Fe−N−O plane) and the d_{yz} orbital of iron.[9] Corresponding bonding ($\alpha\langle 118\rangle$) and antibonding ($\alpha\langle 126\rangle$) orbitals are also shown in Figure 2. To calculate accurate spin densities for **IIa**, the B3LYP functional was applied, as pure density functionals tend to clearly overestimate metal−ligand covalencies. Importantly, only a small amount of spin population is obtained on iron (+0.2), which is mostly due to the Fe−NO σ bond, whereas the contribution from the back-bond is small. As shown in Table 1, most spin population is actually located on the coordinated NO ligand, in agreement with the MCD result. Altogether, a satisfactory theoretical description of the six-coordinate complex **II** is obtained. This is also reflected by the calculated N−O stretching frequency, which is in good agreement with experiment. Therefore, complex **II** must be described as the prototype of a low-spin Fe(II)−NO(radical) adduct.

The interesting question is then how this electronic structure changes when going to the five-coordinate complex **I**. The most important difference is that, because of the absence of the sixth ligand, the d_{z^2} orbital strongly decreases in energy.[5] Hence, mixing with π^*_h becomes very strong such that the HOMO $d_{z^2}\_\pi^*_h$ ($\alpha\langle 101\rangle$) has mostly d_{z^2} character (cf. contour in Figure 2, right). Because of mixing with porphyrin orbitals, an additional 18% d_{z^2} occurs in orbital $\alpha\langle 98\rangle$ (π^*_h contribution = 3%). In total, this corresponds to a net transfer of about one-half of an electron to the Fe(II) center. Hence, the complex has noticeable Fe(I)−NO^+ character. This leads to the occurrence of a large amount of positive spin density on iron (cf. Table 1) and explains the **C**-term MCD spectrum obtained for **I**. In agreement with this description, the N−O stretching frequency is shifted to higher energy by ~70 cm^{-1} in **I** compared to **II** (cf. Table 1). On the other hand, the π back-bond is comparable for **I** and **II**, as shown in Figure 2, right.[10] From single-crystal EPR spectroscopy, the spin populations in the related complex [Fe(OEP)(NO)] have been estimated to +0.9 on iron and +0.1 on NO.[11b] Similar values have been obtained in a recent computational study using pure density functionals.[12] However, this would correspond to an almost complete electron transfer from NO to iron, leading to a low-spin Fe(I)−NO^+ with a d^7 configuration on iron. In contrast, the occurrence of the N−O stretching frequency below 1700 cm^{-1} in **I** shows that this is a clear overestimate. This is also not in agreement with the calculations presented here, which show an even distribution of the unpaired electron over the Fe−N−O unit. In a previous DFT study, it was claimed that complex **I** has Fe(III)−NO^- character.[13] This, however, is not in agreement with our experimental and DFT results.

The results presented above are also useful for evaluating the very different EPR spectra of five- and six-coordinate Fe(II)−porphyrin NO adducts.[11] For complex **I**, a characteristic spectrum is observed with hyperfine lines from the nitrogen of NO on the smallest g value g_{min}. The six-coordinate complex **II** shows a broader spectrum, where hyperfine lines are observed for the nitrogens of NO and of the trans-N donor on g_{mid}. In addition, different g values are obtained for these complexes. It was claimed that these differences in the EPR spectra are due to different orientations of the g tensor with respect to the molecular frame.[6,11c] In agreement with these results, our calculations show that the strong Fe−NO σ interaction in **I** mediated by the orbital $d_{z^2}\_\pi^*_h$ orients the g tensor along the Fe−N(O) bond as shown in Table 1. In this case, the axis of g_{min} (the smallest g value) is almost aligned with the Fe−N(O) bond, which leads to the occurrence of the experimentally observed hyperfine lines on g_{min}. In complex **II**, the g tensor is rotated away from the Fe−N(O) bond, with g_{mid} now being closest to the Fe−N(O) and Fe−N(imidazole) axes. Correspondingly, this g value now shows strong hyperfine splittings. We have also calculated Mössbauer parameters (cf. Table 1) and the ^{14}N hyperfine tensor A of the coordinated NO (cf. Table S2, Supporting Information), which show acceptable agreement with experiment, further indicating that a good theoretical description of **I** and **II** is achieved.

Acknowledgment. This work was supported by the Deutsche Forschungsgemeinschaft (DFG, Grant LE 1393/1) and the Fonds der Chemischen Industrie. F.N. acknowledges financial support by the Max Planck Gesellschaft and the DFG (SPP 1137).

Supporting Information Available: Experimental details, UV−vis absorption vs MCD spectra of **I** and **II** including Gaussian fits, IR spectra of **I** and **II**, MO diagram of **II**, and contour plots. This material is available free of charge via the Internet at http://pubs.acs.org.

IC050144K

(10) Small differences in π back-bonding are observed for the β-MOs. The somewhat increased β-back-bond for **I** compared to **II** leads to the transfer of a small additional amount of spin density from NO to iron in **I** relative to **II**. This will be discussed in detail in the forthcoming full paper.

(11) (a) Wayland, B. B.; Olson, L. W. *J. Am. Chem. Soc.* **1974**, *96*, 6037. (b) Hayes, R. G.; Ellison, M. K.; Scheidt, W. R. *Inorg. Chem.* **2000**, *39*, 3665. (c) Patchkovskii, S.; Ziegler, T. *Inorg. Chem.* **2000**, *39*, 5354. (d) Hüttermann, J.; Burgard, C.; Kappl, R. *J. Chem. Soc., Faraday Trans.* **1994**, *90*, 3077. (e) Zhang, Y.; Gossman, W.; Oldfield, E. *J. Am. Chem. Soc.* **2003**, *125*, 16387.

(12) Zhang, Y.; Mao, J.; Godbout, N.; Oldfield, E. *J. Am. Chem. Soc.* **2002**, *124*, 13921.

(13) Rovira, C.; Kunc, K.; Hutter, J.; Ballone, P.; Parrinello, M. *J. Phys. Chem. A* **1997**, *101*, 8914.